

Electromagnetic Formation Flight

Progress Report: July 2002

Submitted to: Lt. Col. John Comtois
Technical Scientific Officer
National Reconnaissance Office

Contract Number: NRO-000-02-C0387-CLIN0001

MIT WBS Element: 6893087

Submitted by: Prof. David W. Miller
Space Systems Laboratory
Massachusetts Institute of Technology

DESCRIPTION OF THE EFFORT

The Massachusetts Institute of Technology Space Systems Lab (SSL) and the Lockheed Martin Advanced Technology Center (ATC) are collaborating to explore the potential for an Electro-Magnetic Formation Flight (EMFF) system applicable to Earth-orbiting satellites flying in close formation.

PROGRESS OVERVIEW

At MIT, work on electro-magnetic formation flight (EMFF) has been pursued on two fronts: the MIT conceive, design, implement and operate (CDIO) class, and the MIT Space Systems Lab research group, as described in the April 2002 progress report.

The CDIO class has completed its first semester performing trades on and preliminary design of a six-degree-of-freedom electromagnetic formation flight testbed, called “ElectroMagnetic Formation Flight of Rotating Clustered Entities,” or “EMFFORCE.” EMFFORCE will utilize electromagnets to control the size and attitude of a cluster of bodies. The MIT Space Systems Lab research staff is supporting the CDIO class with guidance in trades analysis and design.

Recent work has focused on trade analyses for the design of the electromagnets that will be used in the EMFFORCE testbed. These electromagnets will act as actuators, controlling the relative degrees of freedom of the bodies that compose EMFFORCE. **The following report summarizes recent progress on the trades performed in the design of the EMFFORCE actuation system.**

Preliminary Trade Analysis for the Electromagnet Design for the EMFFORCE Testbed

1 Actuation System Overview

The actuation system includes the electromagnet and reaction wheel subsystems. The electromagnet is designed to provide the electromagnetic force and torque used to induce the spin-up of the vehicles in formation, as well as to reject disturbances in the system during steady-state spin. The reaction wheel assembly is designed to provide torque to counteract the torque induced by the electromagnet. Figure 1.2 shows two dipoles at rest in a perpendicular orientation at a separation distance 2m. The arrows represent the direction of the induced forces and torques on the dipoles. Figure 1.3 depicts the spin-up of two dipoles from an initially perpendicular orientation. As current is applied to the dipoles, they begin to move in the direction of the induced forces and torques. The reaction wheel is then used to apply torque to counteract the induced torque. This applied torque is then decreased until the dipoles are in steady-state rotation, aligned along the same axis.

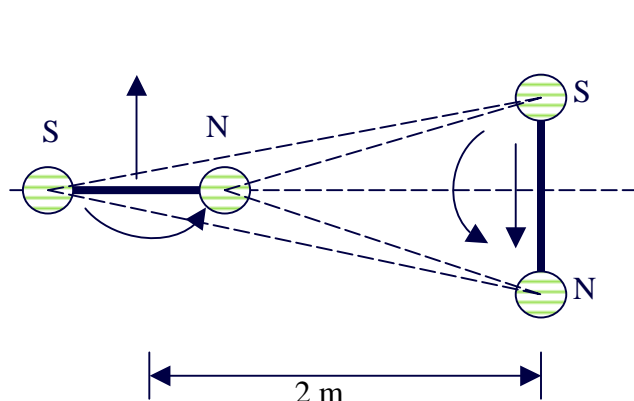


Figure 1.2: Perpendicular Dipoles

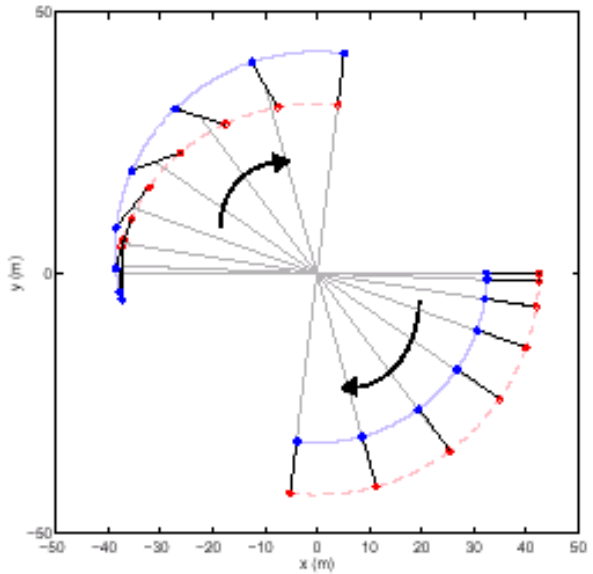


Figure 1.3: Spin-up

2 Purpose of Electromagnet

The amount of force induced by the electromagnet, made up of a solenoid coil and core material, is dependent upon the strength of its magnetic field. The solenoid coil produces a magnetic field when current is applied to it. When the solenoid is wrapped around a ferromagnetic material, this core has the effect of multiplying the strength of the magnetic field.

3 Design Trade Analysis

For the electromagnet, trade analyses were performed to select the core material, core configuration, and mass of the core, coil, and system for the EMFFORCE testbed.

3.1 Core Material

One of the main focuses of the EMFFORCE project is to optimize the amount of force generated by the electromagnet while minimizing its mass. This force depends upon the strength of the induced magnetic field. Therefore, the core material will be selected based on magnetic properties that provide the maximum induced magnetic field at a minimum mass.

When current is applied to a solenoid wrapped around a ferromagnetic core, a magnetic field, or B-field, is induced in the core. As the current is increased, the strength of the B-field increases until it reaches a strength that cannot be exceeded with increasing current. This is known as the saturation value, or $B_{\text{saturation}}$, for a given material. Table 3.1 compares the $B_{\text{saturation}}$ values and densities of several ferromagnetic materials.

Table 3.1: Properties of Magnetic Materials

Material	Composition	$B_{\text{saturation}}$ [Tesla]	Density [g/cm ³]
Iron	99.91% Fe	2.15	7.88
Steel	98.5% Fe	2.10	7.88
45 Permalloy	54.7% Fe, 45.0% Ni	1.60	8.17
78 Permalloy	21.2% Fe, 78.5% Ni	1.07	8.60
Supermalloy	15.7% Fe, 79.0% Ni, 5.0% Mo	0.80	8.77

Iron and steel have the highest values for $B_{\text{saturation}}$ of 2.15 and 2.10 Tesla, respectively. Both iron and steel have the same density, 7.88 g/cm³, which is the lowest among the magnetic materials considered. High $B_{\text{saturation}}$ values combined with lower densities are desirable properties to increase the strength of the induced magnetic field while keeping the mass as low as possible.

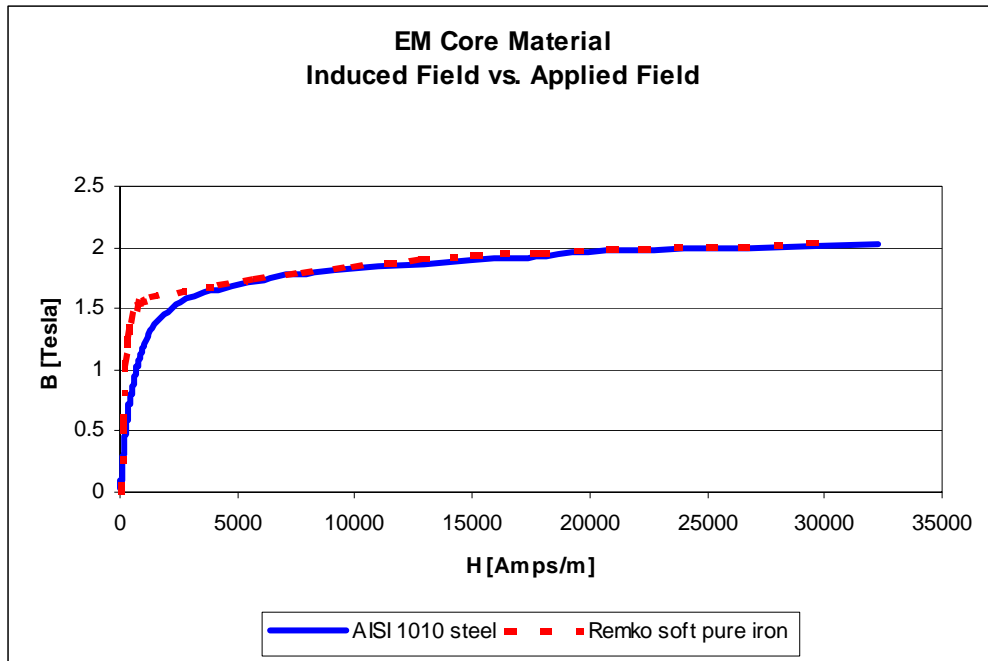


Figure 3.1: Iron and Steel - Induced Field vs. Applied Field

Figure 3.1 is a plot of induced versus applied field for iron and steel. For higher values of the applied field, both iron and steel reach a $B_{\text{saturation}}$ point at approximately 2.1 Tesla. However, for lower values of the applied field, this plot shows that iron has higher induced field values than steel. This is important because it indicates that iron will induce a larger magnetic field, and therefore higher levels of force, than steel at low current levels.

Another magnetic property that must be considered is the hysteresis effect. When a magnetic material is magnetized by an applied field, it will not completely demagnetize when the applied field is reduced to zero. In order to bring the induced field back to zero, a field must be applied in the opposite direction. The strength of this applied field is called the coercive force. The coercive force for iron and steel are 79.6 and 143.2 Amps/m, respectively. Therefore, hysteresis is less of an issue with iron since it requires less of an applied force in the opposite direction to drive the induced field back to zero.

Recently, another possibility for the electromagnet core was discovered. Hiperco 50A, a magnetic alloy made up of 48.9% Fe and 49.0% Co, exhibits better magnetic properties than iron, which was previously the best choice for core material. Table 3.2 shows that Hiperco 50A has a higher value of maximum induced field and requires the same amount of applied field to counter the hysteresis effect.

Table 3.2: Hiperco 50A vs. Iron

Material	B _{saturation} [Tesla]	Coercive Force [Amps/m]
Hiperco 50A	2.40	79.6
Iron	2.15	79.6

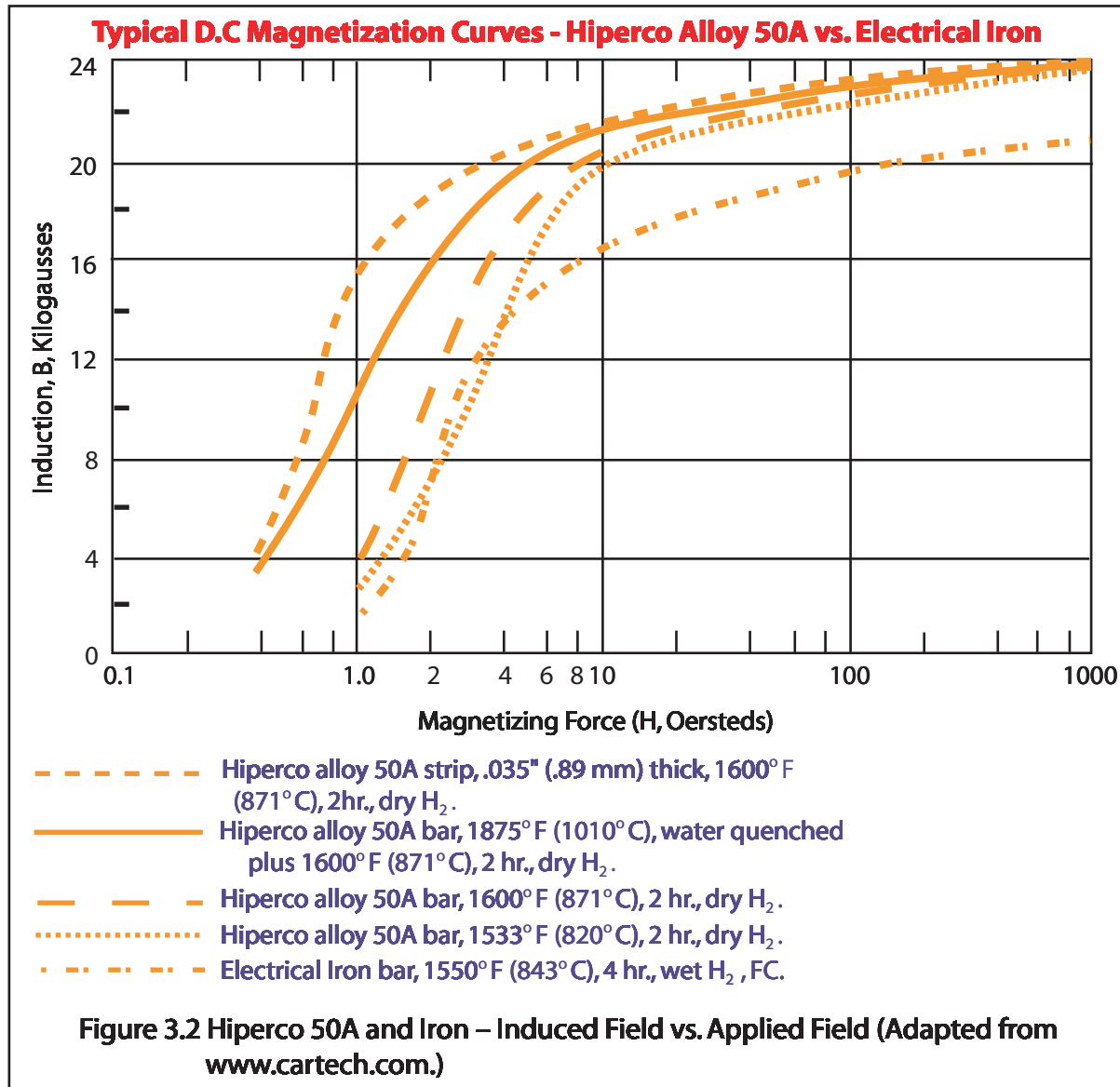


Figure 3.2 shows the relationship between induced field [Tesla] and applied field [Oersteds] for Hiperco 50A and iron. Hiperco 50A has significantly higher values for induced field for a given applied current than iron.

At this time, more analysis is required to determine whether Hiperco 50A is a better choice than iron for the electromagnet core material. Initial analysis indicates that while Hiperco 50A exhibits better magnetic properties than iron, it will be extremely costly to the project and may exceed the electromagnet budget allocation. There are very few distributors of Hiperco 50A, and it will be considerably more expensive to purchase and machine this material than iron.

3.2 Core Configuration

Several preliminary options for the electromagnet configuration on the EMFFORCE testbed have been considered. These include a basic dipole, a Y-pole (3 legs), an L-pole (2 legs connected at their ends), and an X-pole (4 perpendicular legs). All are shown in Figures 3.3-3.6.

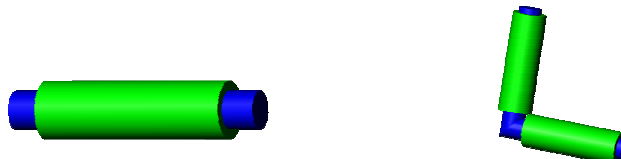


Figure 3.3: Dipole



Figure 3.6: Y-Pole

Before discussing the details of each configuration, it is important to consider the requirements of the system. The reasoning will come in the following section, but for now we assume that our system is driven by its mass. Thus, for a given configuration, if two magnets are at distance between zero and two meters, the mass should be minimized for a given force.

Also, the selected configuration needs to produce the least amount of torque for a given force, since this excess torque must be transferred to the reaction wheel. The reaction wheel's mass will be proportional to the amount of torque that needs to be stored in it, so any unnecessary torque on the system should be minimized.

Finally, there is a requirement that the design of the electromagnet should minimize the effort in transitioning from a two-dimensional testbed to one that operates in three dimensions. This means that the direction of the poles in the magnet should be able to change for the selected configuration.

In order to determine which configuration will satisfy these goals, preliminary calculations were run and a modeling software called “MagNet” was used. From these calculations, the following table was constructed. For each configuration, the performance in several categories is rated between 1 and 5, with 5 being the best performance. The “total” performance of each configuration is summarized in the rightmost column, and it appears the dipole is quite favorable.

Table 3.3: Trades Evaluation for the EMFFORCE Electromagnet Configuration

Trades Config.	Transition to 3D	Minimum mass for a given force	Minimum torque for a given force	Totals
Y-Pole	4	3	2	9
L-Pole	4	2	3	9
Dipole	2	5	4	11
X-Pole	4	1	3	8

In addition to the most important trades summarized in the table, there are some additional arguments against using the L-pole and the X-pole configurations.

The L-pole has a center of mass outside of its own body and would produce adverse torque that would have to be countered by the reaction wheel. Thus using an L-pole would increase the complexity in controlling a body's rotation, since the forces on the system would not be acting through the system's center of mass.

The X-pole was eliminated due to the fact that the mass would have to be distributed to 4 legs. Energizing one of these legs would only be utilizing $\frac{1}{4}$ of the mass that would be used in the single dipole situation and would not produce a large enough force, relatively.

As mentioned before, these are preliminary calculations, and they must be supported with more modeling and testing. However, the favored configurations at this point are the dipole and the Y-pole. In order to determine whether to use a dipole or a Y-pole, it is necessary to compare them closely, with the help of the modeling software.

Two simulations were carried out on the modeling software. In both simulations each configuration has the same volume and mass. The first simulation was with two Y-poles separated by a distance of 2 meters; one leg on each Y-pole was energized with a current of 6 amps through 1200 turns of wire. The energized legs were perpendicular to each other. See Figure 3.7.

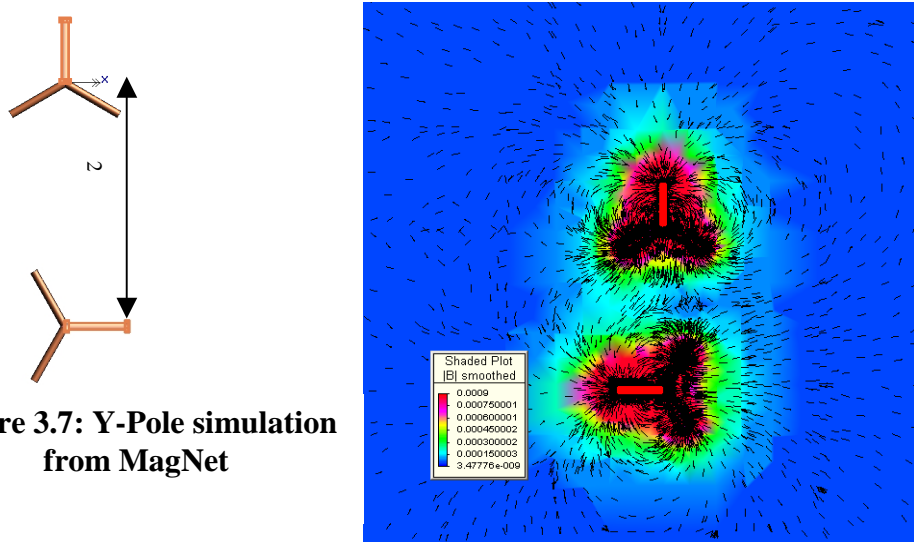


Figure 3.7: Y-Pole simulation from MagNet

For the dipole simulation, two dipoles were used, separated by a distance of 2 meters and perpendicular to each other. Both were energized with a current of 6 amps through 1200 turns of wire. See Figure 3.8.

From the results, the following conclusions can be made:

It was originally believed that the dipole would generate a greater force for a given mass, because for a set core mass, it utilizes the entire core. Also, the Y-pole would not energize the entire core mass at one time and thus it would “waste” some mass. Since the force is what drives the satellites to spin up, this was a key factor.

After running the simulation, it turns out that the Y-pole magnetizes the remaining ends that are not energized and the amount of force generated is greater. This can be explained through Figure 3.7, which shows that the legs on the first Y-pole (that are not energized) are closer to the second Y-pole legs (that are not energized) than are the two dipoles’ main cores.

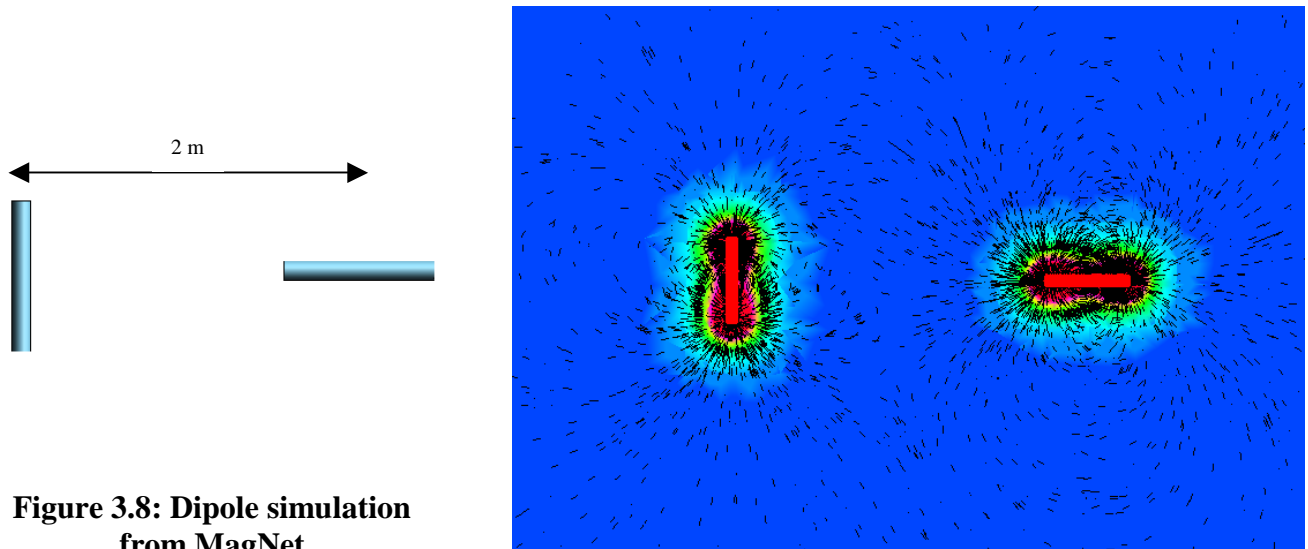


Figure 3.8: Dipole simulation from MagNet

For the requirement of easy transition to three dimensions, it was determined that the dipole cannot change the direction of its poles to an arbitrary direction. The Y-pole, on the other hand, is more versatile and more transitions more easily to three-dimensional applications. This is due to the fact that the Y-pole magnetic field direction can vary by changing the amount of current energizing each of its legs. This would decrease the time it would take to *rotate* an electromagnet to the desired alignment using a reaction wheel. The Y-pole configuration, however, also generates a greater adverse torque than the dipole, which would have to be counteracted by the reaction wheel, making it more massive.

In summary, the Y-pole simulation shows a greater force than the dipole configuration, yet produces more unnecessary torque. The Y-pole performs better in transition to three dimensions and has less mass for a given force than the dipole configuration. However, the torque produced

by the Y-pole is greater than that produced by the dipole; in other words, the dipole performs better in terms of minimizing the amount of torque for a given core mass.

Although it seems that the Y-pole would be the best configuration, this cannot be determined yet. For example, the torque on the electromagnets could be more important than the force on the electromagnets, in which case the performance of the Y-pole and the dipole could change. Since this is unknown, more tests will be run to determine the relations between these factors.

Another possible configuration is a dipole mounted on a rotating disk, so that the direction of the poles could be changed as easily as with the Y-pole. While the dynamics of this system could be more complicated, it will be considered in future trade analyses.

3.3 Core and System Mass

The driving parameter for this design problem is mass. Increases in the total system mass quickly ripple through the system, causing increases in the size of the electromagnet, power system, and structure. Therefore the design of the electromagnet was conducted with the intention of working at the minimum system mass for a given system performance (i.e. separation distance and spin rate).

In order to determine the magnet size, a mathematical model of the system was developed. The total mass of the system is given as:

$$m_{tot} = m_{core} + m_{coil} + m_{power} + m_o$$

Equation 3.1: Total Mass Equation

where the terms are the total mass of the system, the mass of the magnetic core, the mass of the coil of the magnet, the mass of the power system, and the initial system mass, respectively.

Consider the steady-state spin mode, shown in Figure 3.9, where the electromagnets must provide a force that is equal in magnitude but opposite in direction to the centripetal force of the system. The magnetic force on the leftmost vehicle resulting from the other two is given by:

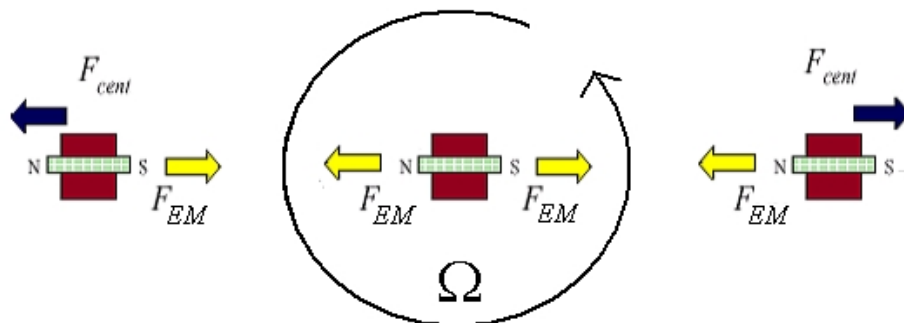


Figure 3.9: Steady State Mode

$$F_{mag} = \frac{3\mu_o\mu_A\mu_B}{2\pi(\frac{s}{2})^4} + \frac{3\mu_o\mu_A\mu_C}{2\pi(s)^4}$$

Equation 3.2: Magnetic Force for Three Vehicles

where s is the separation distance between the two outermost vehicles; μ_a , μ_b , and μ_c are the magnetic moments the three electromagnets, respectively; and μ_o is the permeability of free space. The magnetic force must be set equal to the centripetal force defined by:

$$F_{cent} = \Omega^2 (\frac{s}{2}) m_{tot}$$

Equation 3.3: Centripetal Force

where Ω is the spin rate of the system and m_{tot} is the total mass of a single vehicle.

The magnetic moment of an electromagnet can be approximated as the product of the induced magnetic field (B), the core mass, and the inverse of the core density. Equating Equation 3.2 and 3.3 with this substitution for the magnetic moment and solving for the total mass of the system yields:

$$m_{tot} = \frac{51}{\mu_o s^5} \left(\frac{B m_{core}}{\rho_{core} \Omega} \right)^2$$

Equation 3.4: Total mass in terms of m_{core}

Finding the mass of the other components in Equation 3.1 in terms of the mass of the core yields:

$$m_{coil} = \frac{\rho_{coil} (\pi r_{coil})^2}{i \alpha} \left(\frac{4 m_{core} \alpha^2}{\rho_{core} \pi} \right)^{\frac{2}{3}} H$$

Equation 3.5: Mass of the coil

where the mass of the coil is expressed in terms of the coil radius, the coil density, the current (i), the core aspect ratio (α , defined as the length divided by the diameter), and the applied magnetic field (H). The expression for the battery mass is defined based on the available battery parameters. These equations define the necessary parameters to model the system. The only effect that is neglected in the model is the effect of system mass on the mass of the required structure. This is incorporated into m_o , which has been assumed to be a constant for the current analysis.

This model has been incorporated in a Mathematica script, which can be run to find the optimum operating masses for the system. Before the results of this design are finalized there are a few more factors that must be incorporated. First, it is important to obtain detailed material properties for the core and coil, including B-H curve data for the core material. Also, the model does not yet include an accurate trade between the current and the number of wire wraps. This study will essentially trade between coil mass and battery mass for a given amount of applied magnetic field. Incorporating this trade into the script is anticipated to be a simple step.

Preliminary calculations yield a core mass of ~6.5 kg and a total system mass of ~15 kg. The goal is to reduce the mass as the system design optimization continues.

4 Conclusion

The electromagnet will be composed of a coil and a core. The favored core materials are currently Iron and Hiperco 50A, and the favored configurations are the fixed dipole, Y-pole, and steerable dipole. Further analyses and simulations will be performed in order to downselect the electromagnet materials and configuration, and the optimal number of coil wraps will be determined at that time. All design decisions will be based on the assumption that the success of the system depends largely on reducing mass while still meeting the necessary requirements.